

MUTUAL GENERATIVE TRANSFORMER LEARNING FOR CROSS-VIEW GEO-LOCALIZATION

Jianwei Zhao, Qiang Zhai*, Rui Huang, Hong Cheng

Center for Robotics, UESTC, China

ABSTRACT

Cross-view geo-localization (CVGL), which aims to estimate the geographical location of the ground-level camera by matching against enormous geo-tagged aerial (*e.g.*, satellite) images, remains extremely challenging due to the drastic appearance differences across views. Existing methods mainly employ Siamese-like CNNs to extract global descriptors without examining the mutual benefits between the two modes. In this paper, we present a novel approach using cross-modal knowledge generative tactics in combination with transformer, namely mutual generative transformer learning (MGTL), for CVGL. Specifically, MGTL develops two separate generative modules—one for aerial-like knowledge generation from ground-level semantic information and vice versa—and fully exploits their mutual benefits through the attention mechanism. Experiments on challenging public benchmarks, *CVACT* and *CVUSA*, demonstrate the effectiveness of the proposed method compared to the existing state-of-the-art models. Code will be available.

Index Terms— Cross-view geo-localization, Generative Learning, Transformer

1. INTRODUCTION

Geo-localization provides the geographical location of a street view image which is of paramount importance for autonomous driving [1, 2], robot navigation [3], and routing [4] in a GPS-denied environment. Recent years have seen significant research interest in CVGL as satellite GPS-tagged images are readily available, yet challenging [5] due to the drastic differences in viewpoint and appearance between ground-level optical imagery and aerial-level satellite pattern.

As shown in Figure 1, the existing deep models usually design a two-branch network [6, 7], *i.e.*, Siamese-like model, for learning the higher-order representations from each modality, respectively, and then perform feature similarity estimation to order the most similar matches. However, these models are still incapable of fully resolving the intrinsic visual differences between multi-modal. The Vision Transformer [8, 9] is evaluated as a way to drill down into more representational feature encoding in order to alleviate

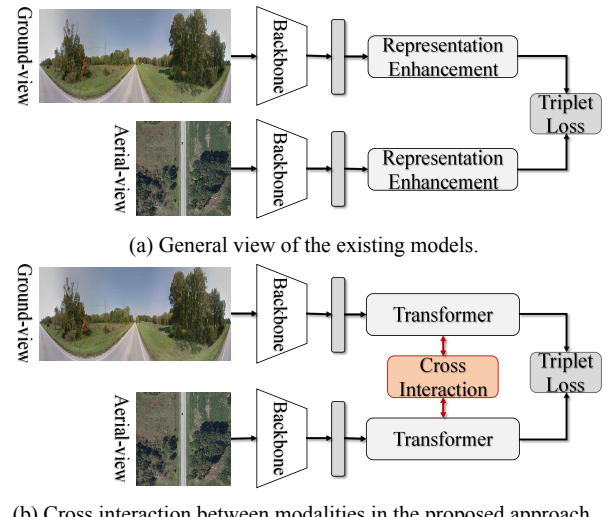


Fig. 1. The **schematic diagram** comparison between the proposed **MGTL** and the existing methods. (a) The existing arts designed Siamese-like deep models to process the ground-level and aerial view images independently, yet they ignore the mutual interaction between the two modalities. (b) The proposed approach further explores interactions cross-modal.

the shortage. Generative Adversarial Network (GAN) [10] brings satellite images closer to ground-level views. Although their remarkable achievements indicate the benefits of establishing *inter-modal* relationships in CVGL, the mutual benefit of *inter-modal* is still poorly explored.

To overcome the shortage, we present a novel Mutual Generative Transformer Learning (MGTL), as shown in Figure 1, to exploit the mutual benefits *inter-modal* for CVGL. Specifically, we carefully design two symmetrical generative sub-modules, *i.e.*, Ground-to-Satellite (G2S) and Satellite-to-Ground (S2G), in a Siamese-like framework to produce the *cross-modal* knowledge, *e.g.*, S2G takes the aerial information and skillfully simulates the ground-aware knowledge, the produced knowledge is further used to enhance the aerial pattern representation under a Transformer-based framework and vice versa. The experiment results on various benchmarks demonstrate the superiority of our proposed model. The contributions of the proposed MGTL can be summarized

*Corresponding author: Qiang Zhai (qiang.zh6@gmail.com)

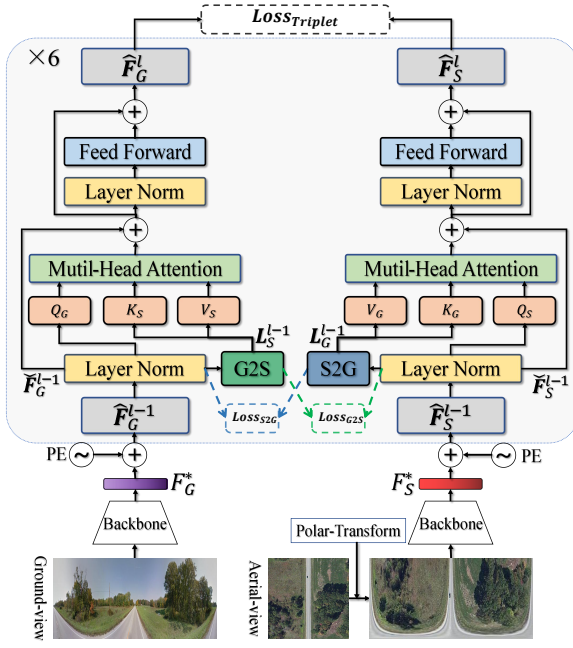


Fig. 2. Overview of the proposed MGTL. MGTL is a Siamese-like deep model contains two *cross-modal* knowledge generative sub-modules, *i.e.*, G2S produces satellite-like knowledge from ground-level information and S2G completes the contrariwise operation. Please refer to § 2 for details.

as follows:

- **A novel cross-modal knowledge guided learning approach for CVGL.** To the best of our knowledge, this is the first tempt to build the mutual interaction between modalities, *i.e.*, ground-level image and aerial-level pattern, in the specified task.
- **Cross-attentive Transformer to exploit the benefits of generative cross-modal knowledge.** Unlike existing Transformer-based CVGL models only can perform *self-attentive* reasoning in the respective modality, our proposed MGTL performs *cross-supported* information to enhance the high-order representation.
- **State-of-the-art localization accuracy on widely-used benchmarks.** Our MGTL outperforms existing deep models on various datasets, *i.e.*, CVUSA [11] and CVACT [12].

2. OUR APPROACH

2.1. Problem Formulation

Let the CVGL model be indicated as the function \mathcal{F}_Θ parameterized by weights Θ , which takes an image pair consists a ground-view image \mathbf{I}_G and a satellite-view image \mathbf{I}_S as input and produces their corresponding representations \mathbf{F}_G and

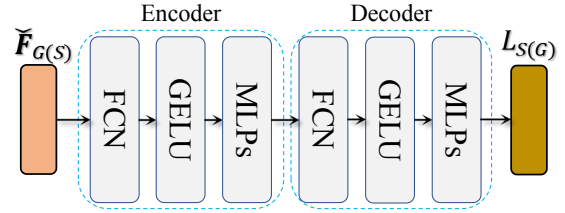


Fig. 3. Illustration of the generative G2S and S2G sub-modules.

\mathbf{F}_S . Our goal is to learn Θ from the labeled training triplets $\{\mathbf{I}_G^i, \mathbf{I}_{SP}^i, \mathbf{I}_{SN}^i\}_{i=1}^M$, where \mathbf{I}_G^i is the ground-view image, \mathbf{I}_{SP}^i and \mathbf{I}_{SN}^i are the positive and negative samples relative to \mathbf{I}_G^i , respectively.

2.2. Mutual Generative Transformer Learning

Our proposed MGTL mainly contains three components: **Modality Independent Feature Extractor (MIFE)**, **Cross-Modality Interaction (CMI)**, and **Generative Knowledge Supported Transformer (GKST)**. Please refer to Figure 2 for the overview.

Modality Independent Feature Extractor (MIFE) f_{MIFE} . f_{MIFE} takes an image pair $\langle \mathbf{I}_G, \mathbf{I}_S \rangle$ as input and produces two modality-specified semantic representations $\langle \mathbf{F}_G^*, \mathbf{F}_S^* \rangle$. Formally, given an image pair $\mathbf{I}_G \in \mathbb{R}^{H_1 \times W_1 \times 3}$ and $\mathbf{I}_S \in \mathbb{R}^{H_2 \times W_2 \times 3}$, a multi-branch backbone (*i.e.*, a Siamese-like VGG-based FCN network with parameters Θ_{MIFE}) is performed to simultaneously extract features for each modality:

$$\mathbf{F}_G^* = f_{\text{MIFE}}(\mathbf{I}_G; \Theta_{\text{MIFE}}), \mathbf{F}_S^* = f_{\text{MIFE}}(\mathbf{I}_S; \Theta_{\text{MIFE}}), \quad (1)$$

where the $\mathbf{F}_G^* \in \mathbb{R}^{c \times h \times w}$ and $\mathbf{F}_S^* \in \mathbb{R}^{c \times h \times w}$ are c channels and $h \times w$ spatial resolution high-order semantic representations for ground-view and satellite-view, respectively.

Cross-modal Interaction (CMI) f_{CMI} . With the purpose of mining the mutual knowledge between multi-modal, CMI takes the information from one modality and produces *another-modality-aware* knowledge. To alleviate the limitation of feature location on learning receptive field, we first re-encode the features \mathbf{F}_G^* and \mathbf{F}_S^* with position information:

$$\hat{\mathbf{F}}_G = \mathbf{F}_G^* + \text{PE}_G, \hat{\mathbf{F}}_S = \mathbf{F}_S^* + \text{PE}_S, \quad (2)$$

where PE_G and PE_S are the positional encoding of feature maps \mathbf{F}_G^* and \mathbf{F}_S^* , respectively. The position-aware representations are further normalized as: $\check{\mathbf{F}}_G = \text{LN}(\hat{\mathbf{F}}_G)$ and $\check{\mathbf{F}}_S = \text{LN}(\hat{\mathbf{F}}_S)$ to maintain representational capacity. Inspired by VAE [13], we design two generative sub-modules f_{G2S} and f_{S2G} with the *encoder-decoder* structure, *i.e.*, shown as Figure 3, to form the cross-modal interaction module f_{CMI} and produce the *cross-modal-aware* knowledge:

$$\mathbf{L}_S = f_{\text{G2S}}(\check{\mathbf{F}}_G), \mathbf{L}_G = f_{\text{S2G}}(\check{\mathbf{F}}_S), \quad (3)$$

Generative Knowledge Supported Transformer (GKST) f_{GKST} . Up till the present moment, we have acquired the

Model	CVUSA				CVACT-val			
	r@1	r@5	r@10	r@1%	r@1	r@5	r@10	r@1%
2015 Workman, <i>et al.</i> [14]	-	-	-	34.30	-	-	-	-
2016 Vo, <i>et al.</i> [15]	-	-	-	63.70	-	-	-	-
2017 Zhai, <i>et al.</i> [16]	-	-	-	43.20	-	-	-	-
2018 CVM-Net [17]	22.47	49.98	63.18	93.62	20.15	45.00	56.87	87.57
2019 Liu, <i>et al.</i> [12]	40.79	66.82	76.36	96.12	46.96	68.28	75.48	92.04
2019 Regmi, <i>et al.</i> [18]	48.75	-	81.27	95.98	-	-	-	-
2019 SAFA [6]	89.84	96.93	98.14	99.64	81.03	92.80	94.84	98.17
2020 CVFT [7]	61.43	84.69	90.49	99.02	61.05	81.33	86.52	95.93
2020 DSM [19]	91.96	97.50	98.54	99.67	82.49	92.44	93.99	97.32
2021 Toker, <i>et al.</i> [10]	92.56	97.55	98.33	99.57	83.28	93.57	95.42	98.22
2021 L2LTR [9]	94.05	98.27	98.99	99.67	84.89	94.59	95.96	98.37
MGTL	94.11	98.30	99.03	99.74	85.35	94.45	96.06	98.48

Table 1. Quantitative results on the *CVUSA* [11] and *CVACT* [12] dataset. Results are cited directly, the best results are highlighted.

intra-modal representation $\check{\mathbf{F}}_G(\check{\mathbf{F}}_S)$ and the generative *cross-modal* knowledge $\mathbf{L}_S(\mathbf{L}_G)$. To learn the final representation \mathbf{F}_G and \mathbf{F}_S , we design a generative knowledge supported transformer (GKST) to fully use all information. Formally, the GKST f_{GKST} takes $\check{\mathbf{F}}_G \in \mathbb{R}^{c \times h \times w}$ ($\check{\mathbf{F}}_S \in \mathbb{R}^{c \times h \times w}$) and $\mathbf{L}_S \in \mathbb{R}^{c \times h \times w}$ ($\mathbf{L}_G \in \mathbb{R}^{c \times h \times w}$) as input and produces the final high-order representations $\mathbf{F}_G(\mathbf{F}_S)$. Taking the ground-view as an illustration, we feed the *intra-modal* representation and *cross-modal* knowledge into a multi-head cross-attention layer to learn the representational features:

$$\begin{aligned} Q_G^i &= \check{\mathbf{F}}_G \mathbb{W}_Q^i, K_S^i = \mathbf{L}_S \mathbb{W}_K^i, V_S^i = \mathbf{L}_S \mathbb{W}_V^i, \\ \text{Head}_i &= \text{Attention}(Q_G^i, K_S^i, V_S^i), \\ \text{MH}(Q, K, V) &= \text{Concat}(\text{Head}_1, \dots, \text{Head}_n), \end{aligned} \quad (4)$$

where \mathbb{W}_Q^i , \mathbb{W}_K^i and \mathbb{W}_V^i are learnable parameters. The updated representations \mathbf{F}_G can be achieved by follows:

$$\begin{aligned} \mathbf{F}'_G &= \text{MH}(Q, K, V) + \check{\mathbf{F}}_G, \\ \mathbf{F}_G &= \mathbf{F}'_G + \text{LN}(\mathbf{F}'_G). \end{aligned} \quad (5)$$

We can easily obtain the final satellite-view feature maps \mathbf{F}_S in a similar way.

Recurrent Learning Process. To fully mine the benefits of the *cross-modal* knowledge, we can further formulate the learning process recurrently as follows:

$$\left\{ \begin{array}{l} \hat{\mathbf{F}}_G^l = f_{\text{GKST}}(\mathbf{L}_S^{l-1}, \check{\mathbf{F}}_G^{l-1}), \mathbf{L}_S^{l-1} = f_{\text{G2S}}(\check{\mathbf{F}}_G^{l-1}), \\ \hat{\mathbf{F}}_S^l = f_{\text{GKST}}(\mathbf{L}_G^{l-1}, \check{\mathbf{F}}_S^{l-1}), \mathbf{L}_G^{l-1} = f_{\text{S2G}}(\check{\mathbf{F}}_S^{l-1}), \end{array} \right. \quad (6)$$

where $\check{\mathbf{F}}_G^{l-1} = \text{LN}(\hat{\mathbf{F}}_G^{l-1})$, $\check{\mathbf{F}}_S^{l-1} = \text{LN}(\hat{\mathbf{F}}_S^{l-1})$. Note that, at the beginning ($l=1$), $\check{\mathbf{F}}_G^0$ and $\check{\mathbf{F}}_S^0$ are produced by Eq. 2, and the final representations \mathbf{F}_G and \mathbf{F}_S are produced by the last layer.

2.3. Implementation Details

Modality Independent Feature Extractor. Following [6], we employ two independent VGG-16 [20] pre-trained

on ImageNet [21] as the backbone and perform the polar-transform on \mathbf{I}_S to make the modality closer to \mathbf{I}_G . We average the feature maps produced by the backbone along height followed by a FCN layer to prepare a more compact feature \mathbf{F}_G^* and \mathbf{F}_S^* with the resolution $384 \times 1 \times 20$.

Cross-modal Interaction. The encoder and decoder are both implemented by two *fully-connected* layers with the GELU activation layer inside.

Loss Function. Following [6], we employ a margin triplet loss for final representation learning:

$$\text{Loss}_{\text{Triplet}} = \log(1 + e^{\gamma(\mathbf{d}_{\text{pos}} - \mathbf{d}_{\text{neg}})}), \quad (7)$$

where \mathbf{d}_{pos} and \mathbf{d}_{neg} indicate the Euclidean distance between the positive and the negative pairs, respectively. The *cross-modal* knowledge generation module is supervised by:

$$\text{Loss}_{\text{Gen}} = \sum_{l=0}^{L-1} (\text{Loss}_{S2G}^l + \text{Loss}_{G2S}^l), \quad (8)$$

where Loss_{S2G}^l and Loss_{G2S}^l are implemented via MSE [22] loss: $\text{Loss}_{S2G}^l = L_{\text{MSE}}^G(\mathbf{L}_G^l, \mathbf{F}_G^l)$ and $\text{Loss}_{G2S}^l = L_{\text{MSE}}^S(\mathbf{L}_S^l, \check{\mathbf{F}}_S^l)$, and L is the recurrent steps. Finally, the overall learning loss is computed as:

$$\text{Loss} = \text{Loss}_{\text{Triplet}} + \lambda \text{Loss}_{\text{Gen}}, \quad (9)$$

where λ is the balancing factor.

3. EXPERIMENTS

3.1. Experimental Setting

Dataset: Following [5, 6, 9], we evaluate the performance on two widely-used challenging benchmarks *i.e.*, *CVUSA* [11] and *CVACT* [12]. Both datasets contain 44416 ground-aerial image pairs and split them into 35532 image pairs for training and 8884 pairs for testing.

Candidate			Complexity		CVUSA				CVACT_val			
VGG16	w/o	w/	FLOPs↓	Param.↓	r@1	r@5	r@10	r@1%	r@1	r@5	r@10	r@1%
✓			4.01G	29.42M	79.94	93.66	96.25	99.31	70.67	87.73	91.13	95.78
✓	✓		4.16G	50.92M	91.42	97.42	98.46	99.63	81.25	92.94	94.81	98.11
✓		✓	4.43G	79.27M	94.11	98.30	99.03	99.74	85.35	94.45	96.06	98.48

Table 2. Ablation study of the proposed approach. 'w/' and 'w/o' means the posed MGTL is or is not equipped with CMI, respectively.

Model	Backbone	Param.↓
L2LTR [9]	ResNet50	195.9M
MGTL	VGG16	72.29M

Table 3. Complexity comparison between L2LTR [9] and the proposed MGTL.

Scene	CMI (L=1)	CMI (L=3)	CMI (L=6)	CMI (L=9)	Naïve (L=6)
CVUSA	r@1	86.44	89.08	94.11	93.81
	r@5	96.20	96.89	98.30	98.28
	r@10	97.74	98.17	99.03	99.02
	r@1%	98.64	99.30	99.74	99.71
CVACT_val	r@1	73.06	80.51	85.35	84.37
	r@5	88.32	92.13	94.45	93.98
	r@10	91.13	94.16	96.06	95.59
	r@1%	95.85	98.01	98.48	98.35

Table 4. Detailed ablation study of different parameter settings. 'L' is the recurrent learning steps.

Evaluation Metric: Following [6, 9], the top- K (r@ K) recall localization accuracy is performed to evaluate our approach. Staying in step with these existing arts, $K = 1, 5, 10, 1\%$ of all the references are selected.

Training Setting: During the training phase, Adam optimizer is used to optimize the network with the learning rate of 10^{-5} . We employ the GKST in 6 recurrent learning steps with 6 heads in each step. We set the batch size to 16 and train the network with 150 epochs. The balancing factor λ is simply set to 0.05, and following [6], the regular item γ in Eq. 7 is set to 10.0.

Reproducibility: We implement the MGTL based on TensorFlow and train the network on a NVIDIA GTX Titan X GPU with 12G CUDA memory.

3.2. Main Results

Baselines: All recently published CVGL models are compared. We totally select 11 STOAs, which are trained under their recommended setting, for omnidirectional comparison.

Performance on CVUSA and CVACT: The comparison results with 11 STOAs on CVUSA [11] and CVACT [12] are shown in Table 1. It shows that our MGTL achieves better performance than all baselines across all metrics on CVUSA

and most metrics on CVACT_val. Our model receives 94.11% and 85.35% top-1 (r@1) retrieval accuracy on CVUSA and CVACT_val, respectively.

3.3. Ablation Study

Effect of Recurrent Learning: Table 4 reports the localization performance under different recurrent learning iterations. Accuracy improved with the increase of learning steps proves that recurrent learning can help to produce a strong representation with the generative *cross-modal* knowledge. However, when further raising the learning steps (L=9), the gains are not noticeable and even go down. As increasing of the learning steps, the quantity and quality of the new generative knowledge would gradually become more difficult.

Effectiveness of CMI: We carefully study the impact in different settings. When we remove CMI, *i.e.*, 'w/o' in Table 2, and keep the workflow in the Siamese-like network independent, we can observe that the performance degrades significantly. Besides, if we use the *local-receptive* CNNs to produce the generative knowledge, *i.e.*, 'Naïve' in Table 4, the localization accuracy degradation still be observed.

Complexity Analysis of MGTL: Table 2 reports the complexity of our model with different configurations. The fully-equipped model costs 4.43 GLOPs and 79.27M memory. We also compare the complexity with the recent baseline, as shown in Table 3, L2LTR [9] slightly exceeds our MGTL only in the r@5 metric, but it tolerates almost thrice the complexity of our model.

4. CONCLUSION

In this paper, we propose a novel multi-modal learning network, *i.e.*, MGTL, to tackle the cross-view geolocation problem. We build and inject the generative *cross-modal* knowledge into a Transformer-based framework to support *intra-modal* high-order information mining. Sufficient experiments demonstrate that our model can fully benefit from cross-modal and set the new record on several widely-used challenging benchmarks. Our findings suggest that the novel perspective can benefit other multi-modal computer vision problems, such as joint perception of Lidar and vision.

5. REFERENCES

- [1] Sixing Hu and Gim Hee Lee, “Image-based geo-localization using satellite imagery,” *IJCV*, vol. 128, no. 5, pp. 1205–1219, 2020. [1](#)
- [2] Yi Xiao, Felipe Codevilla, Akhil Gurram, Onay Urfalioglu, and Antonio M López, “Multimodal end-to-end autonomous driving,” *TITS*, 2020. [1](#)
- [3] Olivier Saurer, Georges Baatz, Kevin Köser, Marc Pollefeys, et al., “Image based geo-localization in the alps,” *IJCV*, vol. 116, no. 3, pp. 213–225, 2016. [1](#)
- [4] Janine Thoma, Danda Pani Paudel, Ajad Chhatkuli, Thomas Probst, and Luc Van Gool, “Mapping, localization and path planning for image-based navigation using visual features and map,” in *CVPR*, 2019, pp. 7383–7391. [1](#)
- [5] Sijie Zhu, Taojiannan Yang, and Chen Chen, “Vigor: Cross-view image geo-localization beyond one-to-one retrieval,” in *CVPR*, 2021, pp. 3640–3649. [1, 3](#)
- [6] Yujiao Shi, Liu Liu, Xin Yu, and Hongdong Li, “Spatial-aware feature aggregation for image based cross-view geo-localization,” *NeurIPS*, 2019. [1, 3, 4](#)
- [7] Yujiao Shi, Xin Yu, Liu Liu, Tong Zhang, and Hongdong Li, “Optimal feature transport for cross-view image geo-localization,” in *AAAI*, 2020. [1, 3](#)
- [8] Alexey Dosovitskiy, Lucas Beyer, Alexander Kolesnikov, Dirk Weissenborn, Xiaohua Zhai, Thomas Unterthiner, Mostafa Dehghani, Matthias Minderer, Georg Heigold, Sylvain Gelly, et al., “An image is worth 16x16 words: Transformers for image recognition at scale,” *arXiv preprint arXiv:2010.11929*, 2020. [1](#)
- [9] Hongji Yang, Xufan Lu, and Yingying Zhu, “Cross-view geo-localization with layer-to-layer transformer,” *NeurIPS*, vol. 34, 2021. [1, 3, 4](#)
- [10] Aysim Toker, Qunjie Zhou, Maxim Maximov, and Laura Leal-Taixé, “Coming down to earth: Satellite-to-street view synthesis for geo-localization,” in *CVPR*, 2021, pp. 6488–6497. [1, 3](#)
- [11] Scott Workman, Richard Souvenir, and Nathan Jacobs, “Wide-area image geolocation with aerial reference imagery,” in *CVPR*, 2015, pp. 3961–3969. [2, 3, 4](#)
- [12] Liu Liu and Hongdong Li, “Lending orientation to neural networks for cross-view geo-localization,” in *CVPR*, 2019, pp. 5624–5633. [2, 3, 4](#)
- [13] Diederik P Kingma and Max Welling, “Auto-encoding variational bayes,” *arXiv preprint arXiv:1312.6114*, 2013. [2](#)
- [14] Scott Workman and Nathan Jacobs, “On the location dependence of convolutional neural network features,” in *CVPRW*, 2015, pp. 70–78. [3](#)
- [15] Nam N Vo and James Hays, “Localizing and orienting street views using overhead imagery,” in *European conference on computer vision*. Springer, 2016, pp. 494–509. [3](#)
- [16] Menghua Zhai, Zachary Bessinger, Scott Workman, and Nathan Jacobs, “Predicting ground-level scene layout from aerial imagery,” in *CVPR*, 2017. [3](#)
- [17] Sixing Hu, Mengdan Feng, Rang MH Nguyen, and Gim Hee Lee, “Cvm-net: Cross-view matching network for image-based ground-to-aerial geo-localization,” in *CVPR*, 2018, pp. 7258–7267. [3](#)
- [18] Krishna Regmi and Mubarak Shah, “Bridging the domain gap for ground-to-aerial image matching,” in *CVPR*, 2019, pp. 470–479. [3](#)
- [19] Yujiao Shi, Xin Yu, Dylan Campbell, and Hongdong Li, “Where am i looking at? joint location and orientation estimation by cross-view matching,” in *CVPR*, 2020. [3](#)
- [20] Karen Simonyan and Andrew Zisserman, “Very deep convolutional networks for large-scale image recognition,” *arXiv preprint arXiv:1409.1556*, 2014. [3](#)
- [21] Jia Deng, Wei Dong, Richard Socher, Li-Jia Li, Kai Li, and Li Fei-Fei, “Imagenet: A large-scale hierarchical image database,” in *CVPR*, 2009, pp. 248–255. [3](#)
- [22] Peter Christoffersen and Kris Jacobs, “The importance of the loss function in option valuation,” *Journal of Financial Economics*, vol. 72, no. 2, pp. 291–318, 2004. [3](#)